ELSEVIER

International Journal of Mass Spectrometry 221 (2002) 39–58

International Journal of Mass Spectrometry

www.elsevier.com/locate/ijms

Recent developments in atmospheric pressure MALDI mass spectrometry

Vladimir M. Doroshenko*, Victor V. Laiko, Nelli I. Taranenko, Vadym D. Berkout, H. Sang Lee

MassTech Inc., Subsidiary of SESI, 4032-A Blackburn Lane, Burtonsville, MD 20866, USA

Received 8 April 2002; accepted 21 July 2002

Abstract

A new atmospheric pressure (AP) matrix-assisted laser desorption/ionization (MALDI) ion source that includes an extended capillary for delivery of AP-MALDI ions toward a mass spectrometer (MS) atmospheric pressure interface inlet aperture, an optical fiber for laser energy transfer to a target, and *x–y* travel stages for high throughput analysis of multiple samples, is described. The new source has been interfaced with a Thermo Finnigan LCQ ion trap mass spectrometer bringing powerful high throughput tandem MS capabilities to MALDI analysis. The resulting AP-MALDI-LCQ instrument demonstrated an absolute sensitivity in the low femtomole range for simple peptide mixture analysis, a mass range up to 2000–4000 (limited by LCQ), and an extensive fragmentation of singly-charged AP-MALDI ions in MS/MS experiments. The potential strength of this technique has been illustrated by numerous applications ranging from fragile molecule analysis to tryptic digest analysis for protein identification. (Int J Mass Spectrom 221 (2002) 39–58)

Keywords: Matrix-assisted laser desorption/ionization; Atmospheric pressure MALDI; Ion trap mass spectrometry; Tandem mass spectrometry; Protein digest

1. Introduction

Two major techniques have been typically used for producing gas phase ions of large biomolecules: electrospray ionization (ESI) [1], and matrix-assisted laser desorption/ionization (MALDI) [2,3]. MALDI is very suitable for analyzing analyte mixtures since it, in contrast to ESI, normally generates singly-charged ions. The principle of MALDI is based on a low melting point of substrate (matrix) doped with analyte compound. Under pulsed laser irradiation (usually in the ultraviolet, or UV spectral region) the matrix material evaporates easily and transports the analyte molecules to the analyzed region of the mass spectrometer (MS) with minimal damage or dissociation (fragmentation) of the analyte. A charging of analyte molecules occurs during pulsed laser-induced desorption. This technique has been successfully applied to many classes of biomolecules [4] such as proteins, peptides, glycoconjugates, carbohydrates, and oligonucleotides, as well as to some synthetic polymers.

The pulsed nature of both the MALDI technique and time-of-flight (TOF) mass spectrometers perfectly complements each other and it is not surprising that most MALDI published results have been obtained on

* Corresponding author. E-mail: dorosh@apmaldi.com

1387-3806/02/$ – see front matter
PII S1387-3806(02)00893-X

a MALDI-TOF instrument [4]. Recent developments of MALDI-TOF-MS have been promoted by the introduction of time-lag focusing [5] to the MALDI process for initial ion velocity correction [6–9], that in conjunction with the use of the reflectron TOF (reTOF) technique [10] results in an increase of mass resolution over 10,000. One major drawback of using time-delayed extraction for the correction of initial velocity distribution is that it is mass-dependent [5], which is problematic for a TOF mass spectrometer intended to record the entire mass range simultaneously.

During the last several years substantial progress has been made towards improving the mass range and resolution of MALDI-TOF mass spectrometry specifically for the analysis of biopolymers and oligonucleotides. High concentrations of buffers and other components, common in real analyte solutions, can interfere with the desorption/ionization process of analytes. The removal of alkali counterions has proven to be very important for achieving high desorption efficiency and mass resolution for all wavelengths and matrices. This removal can be done by the addition of cation-exchange resin beads [11] or volatile ammonium salts such as ammonium citrate or ammonium acetate to the analyte solution [12,13]. On-probe purification using nitrocellulose or modified Nafion film substrates has also been described in the literature [14,15]. The use of wavelengths other than UV was also explored. Infrared (IR)-MALDI-mass spectrometry (MS) [16] was introduced shortly after the discovery of conventional UV-MALDI-MS. In many cases IR-MALDI was shown to be superior to UV-MALDI mostly due to its softness and, as a result, lesser analyte ion fragmentation [11,17–19]. In addition, there are many more potential matrices for IR-MALDI due to the strong absorption of molecular compounds in the IR spectral region; even the correlation between ion formation and matrix absorption in IR-MALDI is not clear yet [20].

Conventional MALDI is a vacuum ionization technique in which sample ionization occurs under vacuum conditions inside a mass spectrometer. In another class of ionization methods, referred to as atmospheric pressure ionization (API) sources, the ionization takes place at normal atmospheric pressure (AP) outside the mass spectrometer. An atmospheric pressure interface is then used to transfer ions into a high vacuum of the mass analyzer. While the transfer of ions from the AP conditions to the vacuum of an MS instrument necessarily introduces ion losses, the total ion yield in the AP ion source is normally higher due to fast thermal stabilization at atmospheric conditions. The real advantage of an AP ion source is the simple introduction of a sample into a mass spectrometer and the direct “on-line” coupling of other analytical separation techniques, such as high performance liquid chromatography (HPLC) or capillary electrophoresis (CE), to the mass spectrometer.

ESI was originally developed as an API source while MALDI, until recently, was exclusively a vacuum ion source, thus, only ESI enjoyed the role of being an on-line HPLC detector. This is despite the fact that these two ionization techniques complement each other in many cases. The advantages of MALDI include simplicity of probe preparation, stability, and a high tolerance to sample contamination. The situation has changed with the invention of AP-MALDI [21,22]. In the AP-MALDI ion source the ions are produced at *normal* atmospheric pressure in contrast to the conventional MALDI ion source where ions are formed inside the *vacuum* system of the mass spectrometer. The operation at atmospheric pressure immediately eliminates the complicated procedure of introducing the sample probe into the high vacuum of the mass spectrometer. Instead, AP-MALDI ions are transferred into the instrument using methods similar to those developed for introduction of ESI ions. The AP-MALDI-MS demonstrated large tolerance to the laser fluence variations (which is beneficial for automated MS analysis), and minimal fragmentation of molecular ions (which is even lower than that in conventional IR-MALDI-MS). In addition, it demonstrated superior data quality for multicomponent peptide mixture analysis compared with conventional MALDI. Clustering between matrix and analyte ions is typically observed in AP-MALDI spectra but these unwanted adduct ions can be partially eliminated by increasing the laser energy or tuning atmospheric

pressure interface parameters [23]. In the initial experiments [21,22], an Applied Biosystems Mariner ESI-TOF-MS was combined with an AP-MALDI source. Recently, Thermo Finnigan LCQ [23,24] and Bruker Esquire [25] ion trap mass spectrometers were interfaced with an AP-MALDI ion source. Peptide ions produced by AP-MALDI could be detected over the entire mass range of the instrument (4000 Da). In the ion trap conditions, the detection of 50 fmol of a peptide loaded on the probe has been demonstrated. Recently, an IR laser operated at 3 μm was used in AP-MALDI source resulting in generation of peptide ions from water and glycerol solutions deposited on the target surface in the form of liquid droplets [26].

In a related study a *laser spray* technique was used for interfacing liquid chromatography (LC) with a mass spectrometer [27,28]. The authors used explosive vaporization and mist formation that occurs when aqueous solution effusing from the tip of the stainless steel capillary (0.1 mm internal diameter) was irradiated by a 10.6 μm CO_2 continuously working infrared laser. Other arrangements were similar to those in ESI experiments. The flow rate was about 100 μL/min. Under the experimental conditions used, the laser spray in general gave stronger ion signals than electrospray. The mechanism of ion formation in laser spray and ESI sources seems to have many common features. As in ESI, the laser spray ion source generates mostly multiple-charged ions. However, additional evaporation in the laser spray results in spraying smaller droplets compared to the ESI case.

In another development, MALDI ions were generated at sub-atmospheric pressures up to several torrs (this is the intermediate case between the vacuum and AP-MALDI) and analyzed using orthogonal acceleration (oa)-reTOF-MS [29–31]. When the collisional cooling in the rf quadrupole ion guide at the pressures of the order of 10^{-2} Torr is used [30] the features of MALDI mass spectra are not very different from those in a conventional vacuum MALDI-MS. Increasing the pressure up a few torrs improved the stability of peptide and protein ions so that losses of small groups and backbone fragmentation were practically eliminated [31]. Higher gas pressure in the MALDI ion source introduced additional losses in the ion transport system and caused substantial cluster formation. The clustering and ion losses were less severe with the use of volatile matrices (water–alcohol), CO_2 laser at $\lambda = 10.6$ μm, and a high electric field in the ion source. Increasing the temperature of the API interface also eased the problem of cluster formation for peptide and protein ions. Despite the presence of features which are distinct to AP-MALDI, a sub-AP-MALDI source is still a vacuum ion source since it requires an introduction of samples into a pumped chamber before analysis.

In this paper, we describe the further development of AP-MALDI technique including the use of an extended capillary for delivering ions toward an inlet aperture of a mass spectrometer and linear translation stages for automated high throughput analysis of MALDI sample arrays. Optimization of the source parameters is described and AP-MALDI data obtained for some applications are presented.

2. Experimental

2.1. AP-MALDI-MS interface

Experiments were performed on a Thermo Finnigan (San Jose, CA, USA) LCQ Classic ion trap mass spectrometer integrated with a MassTech Inc. AP/MALDI® ion source prototype as shown in Fig. 1. The AP-MALDI source housing consisting of two aluminum cap-like flanges replaces an LCQ ESI source. An optical flange bolted to the LCQ inlet flange holds major optical elements for directing and focusing a laser pulse delivered by an optical fiber cable and allows viewing of a sample using a CCD camera. A target flange contains a target plate with multiple samples on it and *x* and *y* linear translational stages for moving samples into a working position. The optical flange is mounted on the LCQ inlet flange using standard bolt holes and the target flange is placed onto the LCQ sliding platform so

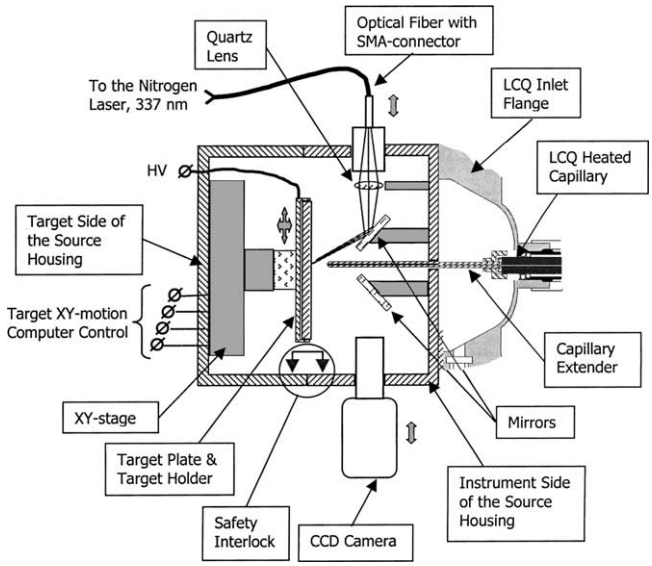

Fig. 1. A scheme of the atmospheric pressure MALDI ion source interfaced with an LCQ ion trap mass spectrometer.

that two flanges can be connected with each other in the operational position and are slid apart for sample target change or maintenance.

In previous AP-MALDI experiments [21–23] the sample was located in close proximity (usually 1–2 mm) to the inlet hole of the atmospheric pressure interface of the mass spectrometer. In the AP/MALDI design, the optical flange mounted on the LCQ inlet flange includes an extended capillary to transfer ions formed on the target plate toward an LCQ atmospheric pressure interface capillary inlet hole. The design allows two capillaries to be sealed at the place of the connection using a Teflon gasket. The extended capillary is made of a 50 mm long stainless steel tubing having a 1.5 mm outer diameter and an 825 μm inner diameter that is about two times larger than the LCQ inlet capillary internal diameter. The edge of the extended capillary tip was sharpened from the outer side at about a 30° angle. Due to the larger inner diameter, the extension capillary does not introduce a substantial pressure drop to the inlet gas flow. Thus, the gas pressure at the LCQ inlet hole remains approximately the same as before the LCQ modification that ensures undisturbed operation of the modified LCQ atmospheric pressure interface. The extra space provided by the extended capillary is required for mounting an optical lens and mirrors since the AP/MALDI design uses a large (about 38 mm × 38 mm) target plate for analyzing multiple (up to 64) samples. The tip of the extended capillary is placed next to the target surface at a distance of about 2 mm unless otherwise specified.

A Thermo Laser Science Inc. (Franklin, MA, USA) Model 337 Si nitrogen UV laser (wavelength $\lambda = 337$ nm, laser pulse duration is about 4 ns) has been used for desorption of ions from the MALDI sample. The laser beam was focused on the end of an optical quartz glass fiber cable. The other end of the 2-m long optical cable was connected to the optical flange of the AP/MALDI source. The optical channel used for directing and focusing the laser pulse from the fiber end onto the target includes a 25-mm focal length quartz lens and an aluminum-coated turning mirror (see Fig. 1). The beam was focused on the target area closest to the extended capillary inlet tip. The beam incidence angle was approximately 45°. The laser fluence was controlled by focusing/defocusing the laser beam on the target. A sample and laser spots were observed on a video monitor using a CCD camera with

total magnification of about 100×. The viewing angle was about 45° toward the target surface. The viewing channel consists of a turning mirror and a relay lens for imaging the sample onto the CCD camera's sensitive area. The size of a laser spot was measured on the video monitor using dark traces left after matrix depletion on the target surface covered with the CHCA matrix (see below). Typical size of the laser spot during the operation was about 0.5 mm. The maximum laser energy on the target measured directly at the target using a Molectron Detector (Portland, OR) Model EM-400 laser energy meter equipped with a Model J8LP pyroelectric probe, was in the 50–150 μJ/pulse range.

The gold-plated steel target plate in the AP/MALDI source was placed atop the crossed *x* and *y* linear motorized stages (National Aperture Inc., Salem, NH, USA) controlled via a computer serial RS-232 port using MassTech's software. The software allowed full control of the target plate position relative to the extended capillary tip. When the sample is consumed by laser-induced desorption the software allows one to continuously move the sample plate along the spiral line to expose a fresh sample for every laser shot. Using this technique, the time for analysis of the same sample could be extended up to 1 h. In order to facilitate the migration of ions toward the extended capillary inlet, the target plate was placed under high voltage varying in the 1.5–3 kV range (provided by the LCQ instrument—the needle voltage in the ESI ion source). In order to minimize ion losses while they are transferred to the mass analyzer, the AP-MALDI chamber is filled with dry nitrogen (not shown in Fig. 1, supplied from the LCQ lines).

The AP/MALDI electronics and software provide simple handshaking communication for interaction with the LCQ Xcalibur control software. For example, the trigger pulse can be supplied for the LCQ to start the data acquisition process. Similarly, the LCQ's contact closure status can be read by the AP-MALDI software for the start and finish of the laser firing and moving along the spiral line, as well as shifting to the next sample after completion of data acquisition on the current sample. The communication between the LCQ and AP/MALDI electronics is performed via the cable connected to the LCQ Peripheral Control connector.

2.2. Operation and sample preparation

Experiments were carried out in a repetitive laser shot mode with the laser frequency equal to 10 Hz. The laser trigger times were not synchronized with the LCQ operation. The AP-MALDI ions effectively formed a quasi-continuous ion beam at the exit of the LCQ inlet capillary. The temperature of the LCQ capillary was typically held at 250 °C, unless otherwise specified. Typical high voltage applied to the target plate was 2000 V. Optimal LCQ parameters (e.g., ion lens and multipole guide voltages) were found according to a standard LCQ tuning procedure using ESI or AP-MALDI ion sources. Both sources generated similar tuning parameters. The automatic gain control (AGC) option was turned off for all experiments described below with typical injection time set to 500 ms. The spectra presented have been accumulated during the time interval from 30 s to 3 min depending on the analyte concentration. The experiments described in this work were all performed in a positive ion mode.

The samples for mass spectrometric analysis were prepared on the gold-plated target plate by mixing 0.5–1 μL of 0.1% TFA aqueous analyte solution with 0.5–1 μL of a matrix solution. The samples on the target were naturally dried at room temperature. Two different crystalline matrix solutions were used for the UV-MALDI analysis. 2,5-Dihydroxybenzoic acid (DHB) and α-cyano-4-hydroxycinnamic acid (CHCA) were prepared as saturated solutions in the mixture of water and acetonitrile (volume ratio 1:1). The matrices and peptides were purchased from Aldrich (Milwaukee, WI) and Sigma (St. Louis, MO), respectively, and were used without any further purification. Tryptic digest mixtures were purchased from Michrom BioResources (Auburn, CA, USA). The PNA sample was obtained from Max Plank Institute for Molecular Genetics (Berlin, Germany). Substance PNN-82 (see below) was kindly provided by Fidelity Systems Inc. (Gaithersburg, MD, USA).

3. Results and discussion

3.1. Optimization of operational parameters in AP-MALDI experiments

There are several operational parameters related to the AP-MALDI source which need to be optimized to get the best performance. Among them are: high voltage applied to the target plate, temperature of the LCQ capillary (the extended capillary was not heated), the time of injection of ions into the trap, etc. In addition, there are other source design parameters that need to be addressed such as the extended capillary length, distance between the capillary and the target plate, etc.

The dependence of the ion signal upon the ratio of voltage/distance between the target plate and the extended capillary tip is shown in Fig. 2. The measurements were made using Bradykinin as a working compound (600 fmol/sample loaded). Each point is an average of the analyte intensity in four to five spectra obtained from four to five different samples. In order to study the dependence of the ion signal upon the distance between the extended capillary tip and the sample target plate, several sets of experiments were conducted with the extended capillaries having a slightly different length. Dark and clear circles in Fig. 2 represent the data for distances of 2 and 3 mm, respectively. In general, the ion signal increases with the voltage applied until some value, which is about 3–4 kV depending on the distance between the capillary and the target. It has been shown experimentally by turning off the nitrogen laser that a corona discharge starts playing a role at high voltages. Thus, one can see that the ion signal steadily increases when increasing the voltage due to better transfer of ions from the target to the capillary inlet until the corona discharge starts playing a negative role. Because of the finite value of the extended capillary diameter, the voltage/distance ratio is not the only parameter describing the electric field between the target plate and the capillary tip. However, the data for different distances between the capillary and the target are close to each other in Fig. 2. The biggest discrepancies are observed when high voltages are applied. It can be seen from the data in Fig. 2 that using smaller distances between the target and the capillary can result in a higher ion signal.

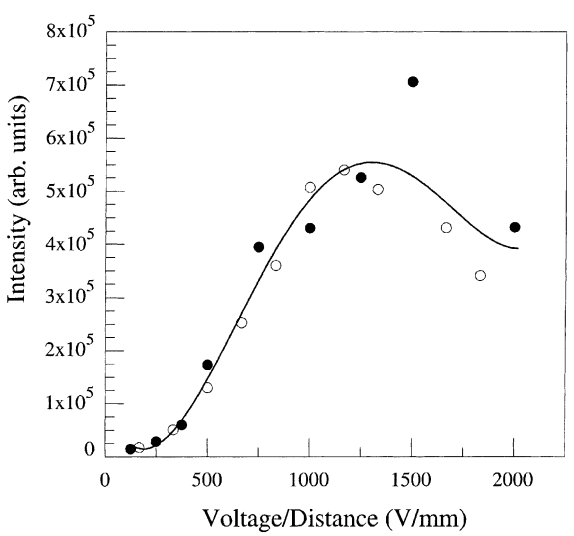

Fig. 2. The dependence of Bradykinin (MW 1060.2 Da) molecular ion intensity in AP-MALDI spectra upon the ratio of voltage/distance between the extended capillary and the target plate. Dark and clear circles correspond to the distances of 2 and 3 mm, respectively.

The LCQ capillary temperature is another important parameter. It has been reported that the capillary temperature strongly affects the analyte–matrix dissociation process [22,32]. This effect is illustrated by the data shown in Fig. 3(a) and (b) where the AP-MALDI mass spectra of a mixture of peptides were obtained at two capillary temperatures: 200 °C (Fig. 3(a)) and 250 °C (Fig. 3(b)). The 0.6 pmol of each peptide (except [Tyr]-Substance P) were loaded. We assume that [Tyr]-Substance P was formed from regular Substance P by hydroxylation of phenylalanine aminoacid residue due to the long storage time of this peptide. The peaks in Fig. 3(a) corresponding to the molecular ion and analyte–matrix clusters of Bradykinin are designated by (a), those for Angiotensin I, Substance P, its derivative [Tyr]-Substance P, and Fibrinopeptide A are marked by (b), (c), (d), and (e), respectively. Note that the distance between analyte–matrix cluster peaks of the same series is a multiple of 378 Da that corresponds to two CHCA matrix molecules (MW 189 Da). No clusters other than those corresponding

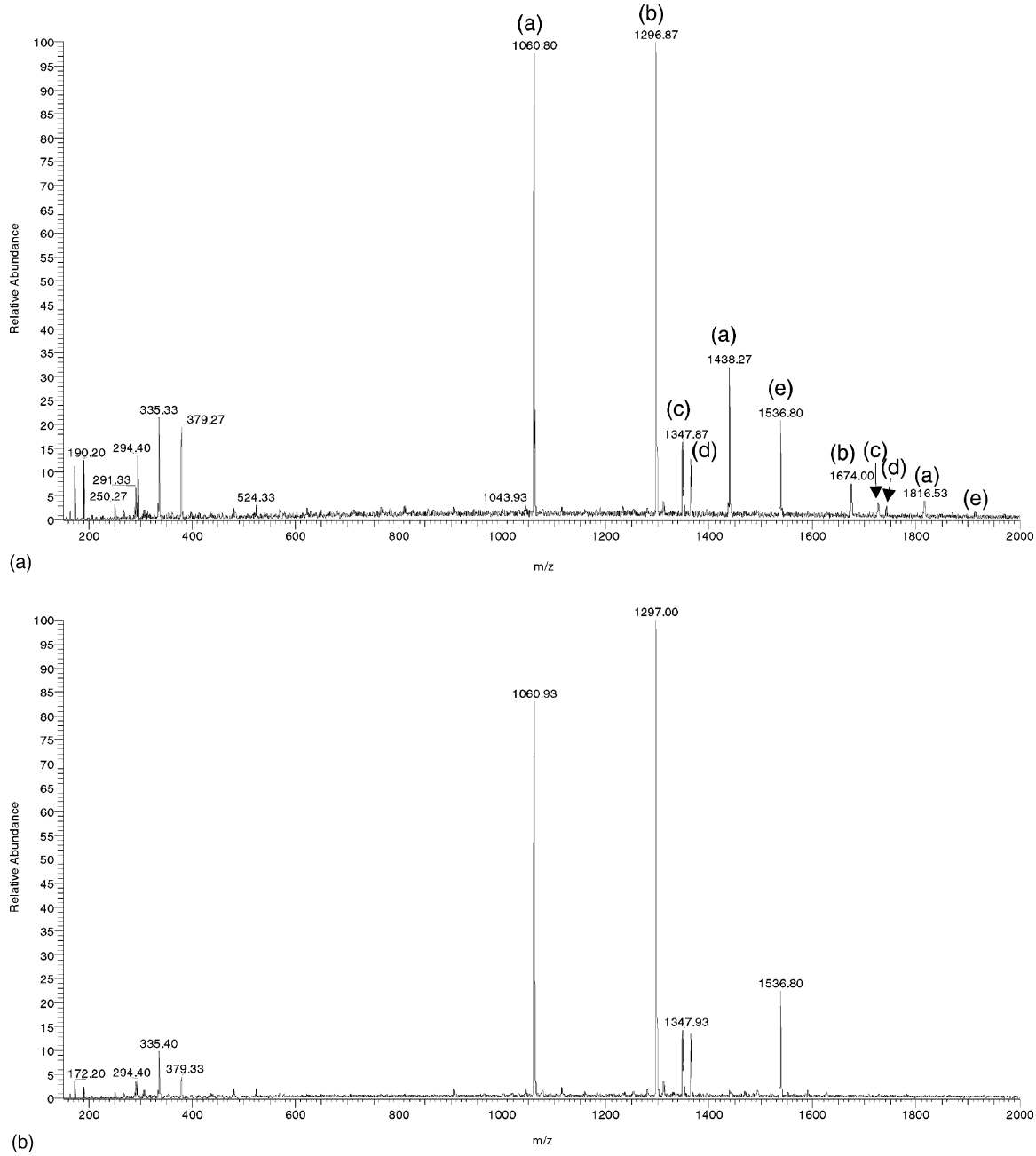

Fig. 3. AP-MALDI mass spectra of mixture of peptides (Bradykinin: MW 1060.2 Da, Angiotensin I: MW 1296.5 Da, Substance P: MW 1347.3 Da, [Tyr]-Substance P: MW 1363.3 Da, and Fibrinopeptide A: MW 1536.6 Da) obtained at different temperatures of the LCQ capillary: (a) −200 °C and (b) −250 °C. CHCA was used as a matrix.

to 2 or 4 CHCA molecules are observed in the spectrum in Fig. 3(a). Similar discrimination in the number of clustering molecules known as a *magic* number phenomenon was observed in mass spectra of clusters of simple molecules [33] and corresponds to a compact molecular cluster structure having minimal formation energy. In our case this may be reflective of well-known tendency of carboxylic acid groups to dimerize in the gas phase. Thus, it is possible that analyte–matrix cluster ions observed in the spectrum in Fig. 3(a) actually correspond to analyte–(matrix cluster) complexes. It is significant that increasing the capillary temperature by 50 °C results in complete elimination of such cluster complexes in the mass spectrum (Fig. 3(b)). It was found that the optimum capillary temperature is about 250 °C which also corresponds to the maximum intensities for molecular ions. Maintaining the optimal temperature is important not only for increasing the AP-MALDI sensitivity but also for unambiguous mixture analysis since at such temperature every mixture component results in a single peak in a mass spectrum. Too high temperatures can result in partial fragmentation of molecular ions (data not shown). There are indications that the optimal capillary temperature depends slightly on the matrix used for sample preparation [32].

The intensity of the molecular ion peak of Angiotensin I from the spectrum in Fig. 3(b) was used to study the dependence of ion peak intensities upon the duration time for injection of ions into the trap. This dependence is shown in Fig. 4. One can see that approximate linear dependence between the peak intensity and the injection time is observed up to 500 ms. The peak intensity barely changes for longer injection times. The injection time of 500 ms is the optimal time for AP-MALDI experiments since duty cycle is lower for smaller injection periods and ions are not effectively used for longer times as seen in the data in Fig. 4. It was noted earlier that in Thermo Finnigan ion traps, the ion signal depends on the laser firing time [24] because the LCQ instrument uses four distinct rf voltage levels for injection of ions in the 100–2000 Da mass range. In our experiments due to the high frequency of laser firing (10 Hz) laser pulses

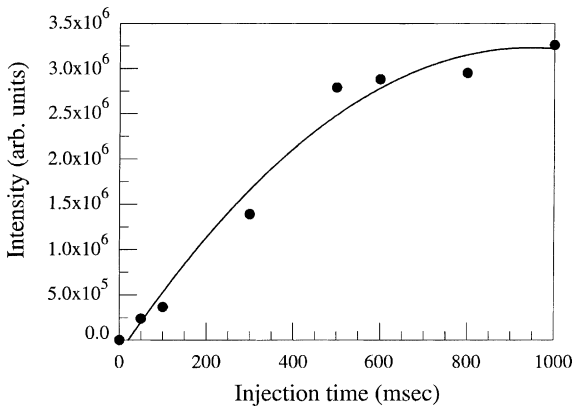

Fig. 4. The dependence of the Angiotensin I molecular ion peak intensity upon the injection time of ions into the trap.

uniformly filled the relatively long injection period and, thus, the synchronization of laser pulses with the ion injection period is not important.

The dependence of the ion signal upon the extended capillary length was studied in special experiments in which the AP/MALDI source was separated from the LCQ instrument and the extended capillary was elongated using additional stainless steel or PEEK tubing of different lengths and the same 825-μm internal diameter. When using PEEK tubing the electric

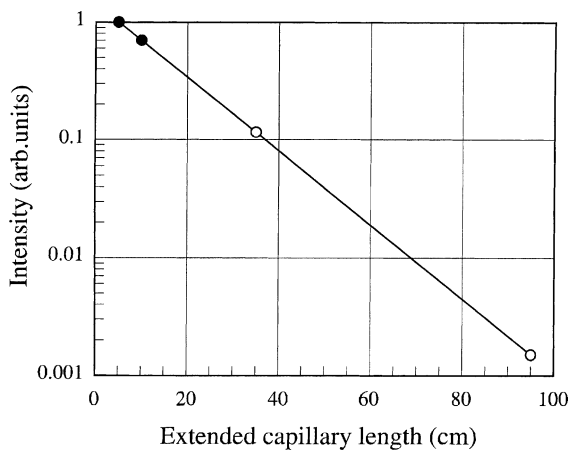

Fig. 5. The dependence of the Angiotensin I molecular ion peak intensity on the length of the extended capillary. Dark and clear circles correspond to the data for the stainless steel and PEEK capillaries, respectively.

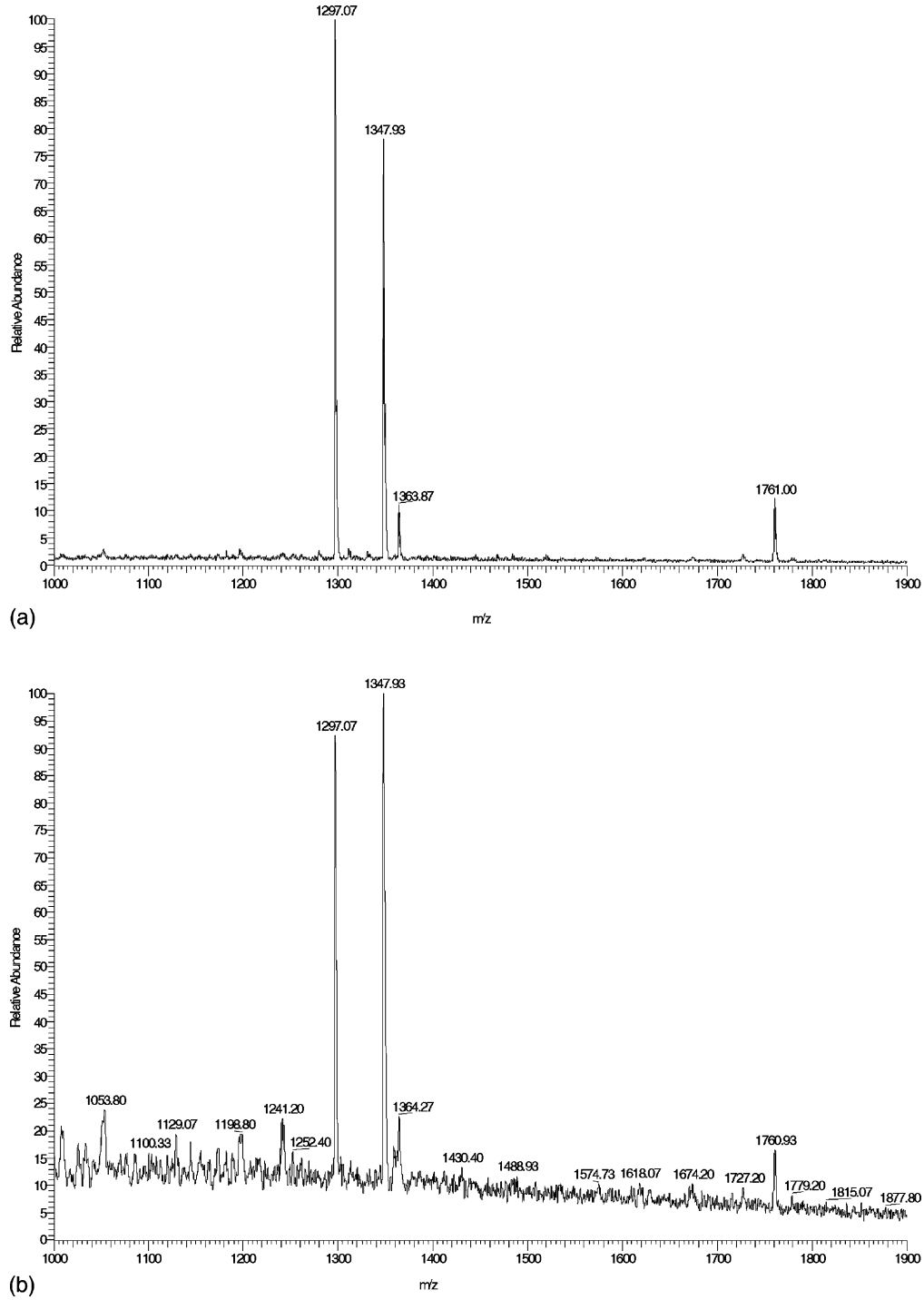

Fig. 6. AP-MALDI mass spectra of peptide mixture for different amount of each peptide loaded to a sample: (a) 100 fmol; (b) 20 fmol; (c) 6.6 fmol; (d) 1 fmol. CHCA was used as a matrix.

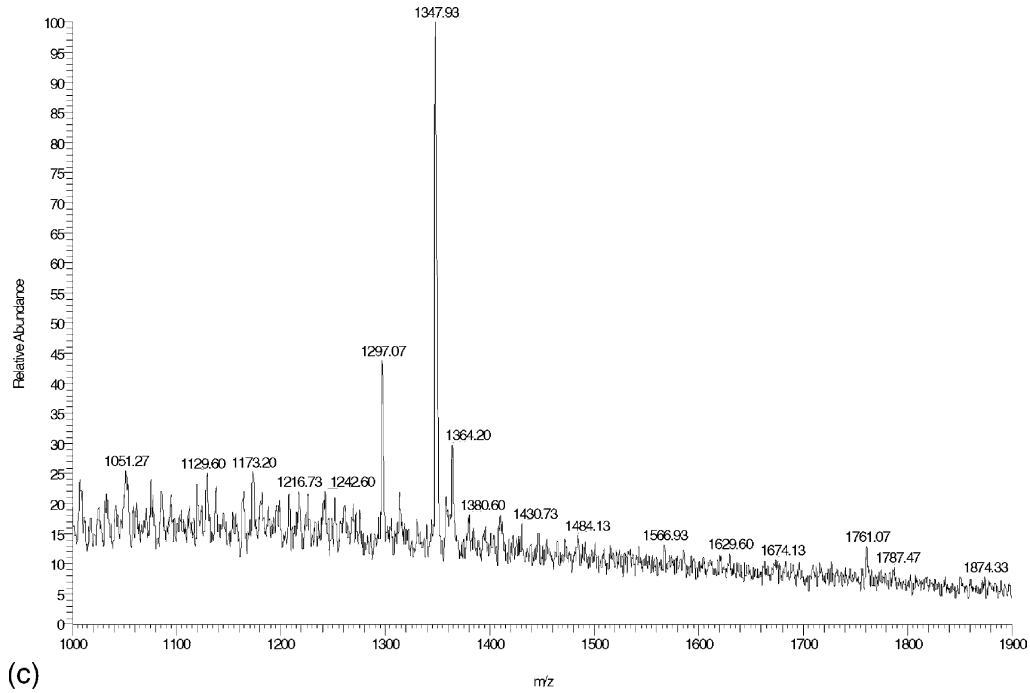

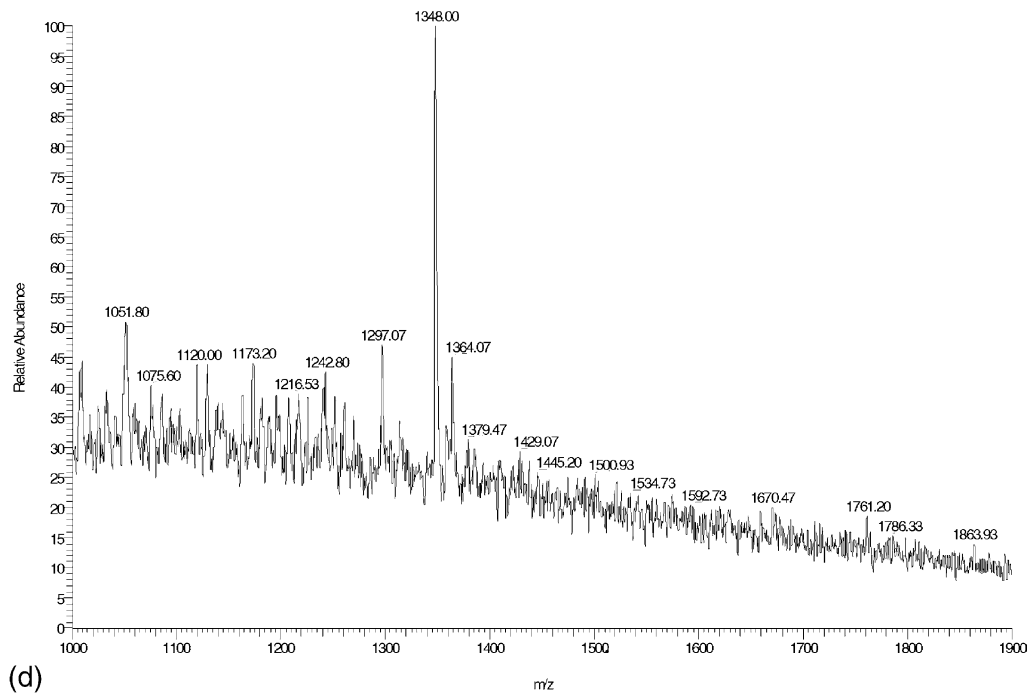

Fig. 6. (*Continued*).

potential on the extended stainless steel capillary tip was maintained at the same level using a wire connecting the tip with the LCQ inlet capillary. The tubings were connected with each other using zero dead volume unions having the channels of the same internal diameter as the tubings. The sealing of the elongated tubing at the LCQ side was the same as before the elongation. The same standard peptide mixture used for obtaining data in Figs. 2 and 3 and the intensity of the Angiotensin I peak in the AP-MALDI spectra was used to study dependence of the ion signal upon the extended capillary length (Fig. 5). As one can see from the data in Fig. 5, there is an exponential dependence of the losses of ions in the extended capillary upon the capillary length. The data obtained using stainless steel and PEEK tubing lie on the same line. One may conclude that the rate of losses of ions on the tubing walls does not depend on the material that the tubing is made of. This conclusion and the rate of losses observed in this work are in a good agreement with the published experimental and theoretical data on transfer of ions through long capillaries [34].

We also studied the dependence of ion signals upon the diameter of the extended capillary by changing the capillary diameter in the range from 500 μm (which is close to the diameter of the LCQ inlet capillary) to 1000 μm. No strong dependence of the ion intensity upon the capillary diameter was observed. The ion signal dropped notably only for the 500-μm diameter capillary (data not shown). This can probably be explained by a poor junction between the LCQ and the extended capillaries due to the close diameters of small capillaries to be connected.

3.2. Mixture analysis using the AP-MALDI source

One of the benefits of using the AP-MALDI source compared to ESI is that in many cases mixtures can be analyzed without prior separation by chromatography or electrophoresis techniques. As a result the time for analysis can be shortened from about an hour to minutes or even seconds. Thus, high throughput can really be achieved using the AP-MALDI technique for mixture analysis.

The concentration limit for simple mixture analysis using AP-MALDI is illustrated by the data shown in Fig. 6(a)–(d) where the mixture of Angiotensin I, Substance P (and [Tyr]-Substance P), and Renin Substrate Tetradecapeptide (MW 1759.0 Da) was analyzed. One can see that all peptides can be seen at the level of

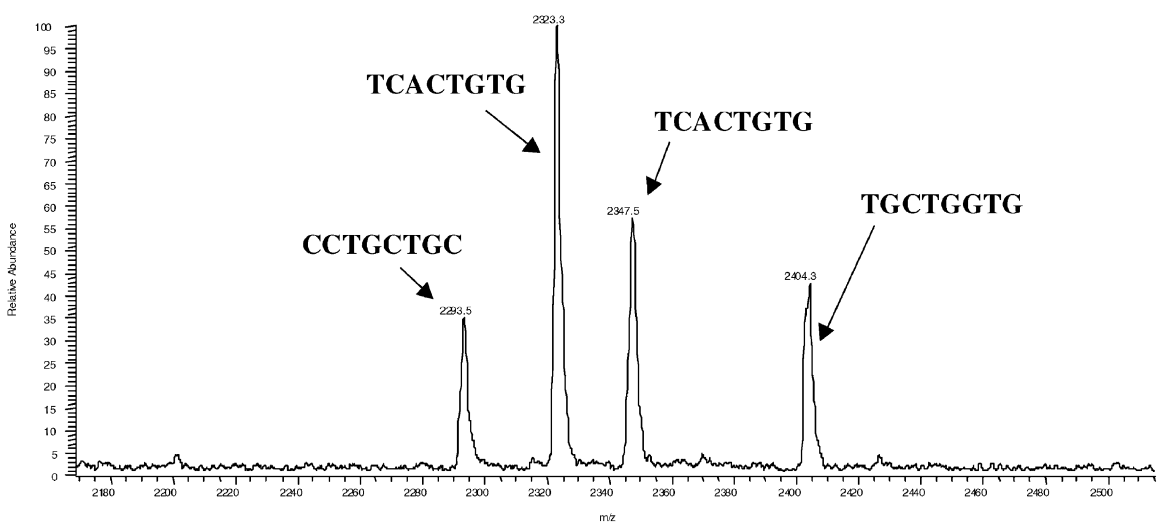

Fig. 7. AP-MALDI mass spectrum of the mixture of PNA molecules. CHCA was used as a matrix (25 fmol of each 8-mer PNA molecule loaded).

1 fmol. Note that the LCQ Classic ion trap mass spectrometer used in this work is less sensitive than the newest LCQ Deca and LCQ Deca XP by about an order of a magnitude. Thus, even low detection limits can be achieved using those instruments.

Another example of mixture analysis is shown in Fig. 7 where the AP-MALDI mass spectrum of mixture of 8-mer peptide nucleic acids (PNAs) is presented. PNAs are a new class of DNA mimics in which the regular nucleobases are connected via

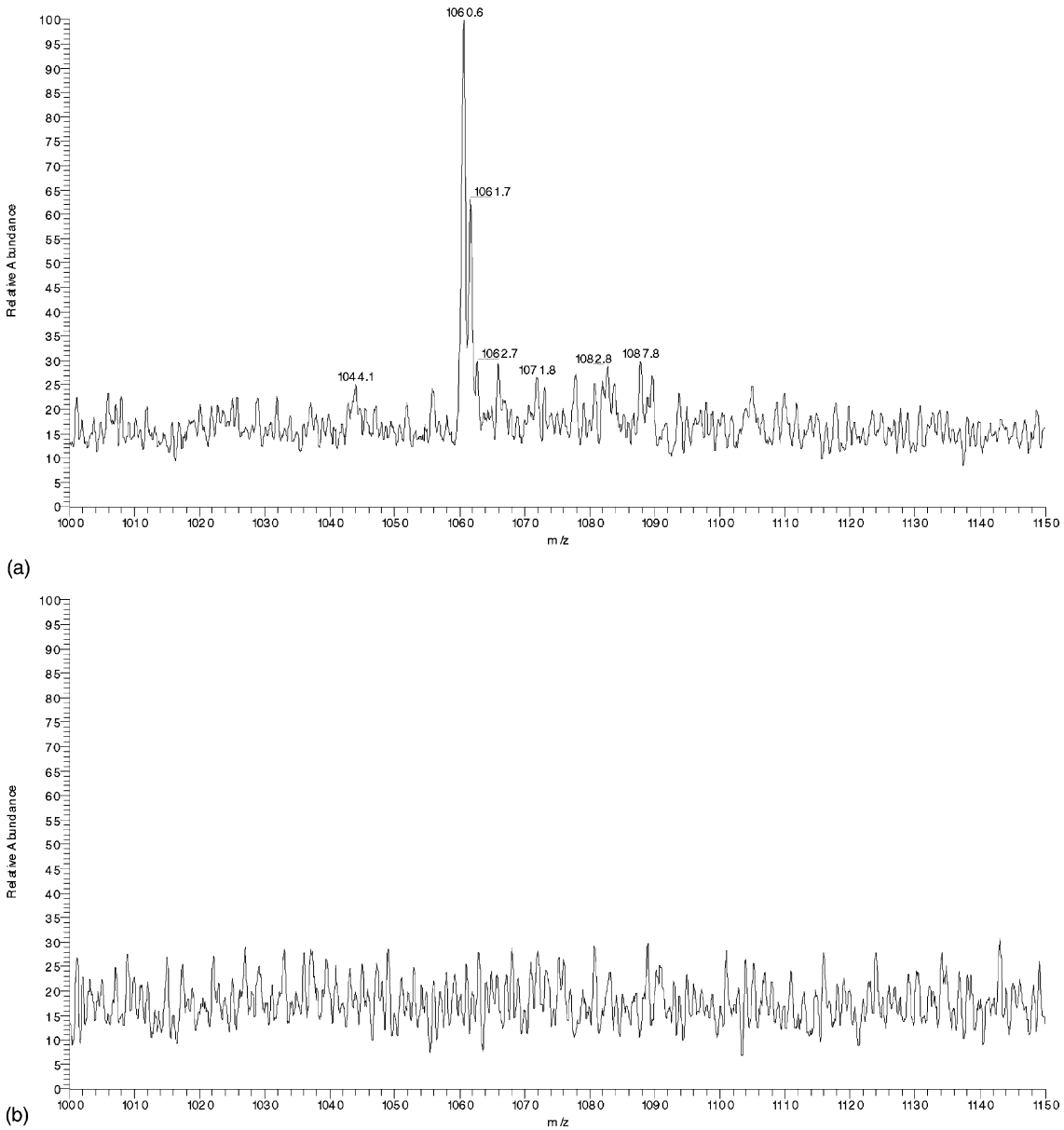

Fig. 8. (a) The AP-MALDI mass spectrum from 150 amol of Bradykinin in CHCA matrix; (b) the spectrum from bare CHCA matrix obtained before the acquisition of the Bradykinin spectrum.

a peptide-like backbone. PNA molecules retain the same Watson–Crick pairing as regular nucleotides, with the added benefits of greater specificity and resistance to enzymatic digestion. PNA molecules can hybridize to complimentary DNA sequences because the nucleobases come off the backbone at equal spacing to the DNA bases.

3.3. Small molecule studies

The AP-MALDI source interfaced with an LCQ ion trap mass spectrometer is especially useful for studies of small molecules since the mass range of the instrument is limited by 2000 or 4000 Da (when proper LCQ Xcalibur control software is installed). The real benefit comes from the $(MS)^n$ capabilities of LCQ opening the way for molecule structure elucidation studies.

AP-MALDI, like a conventional MALDI, discriminates against analyte molecules based on their structure, basicity/acidity, proton affinity, etc. For some favorable molecules it is possible to obtain very low detection limits in AP-MALDI interfaced with LCQ Classic instrument as demonstrated by data in Fig. 8(a) where the AP-MALDI mass spectrum from 150 amol of Bradykinin is shown. A special cleaning procedure of the target surface involving a sonicating bath was used to make sure that the signal did not come from the surface, contaminated from previous experiments. The spectrum from the bare CHCA matrix deposited on the cleaned surface before the spectrum shown in Fig. 8(a) was acquired demonstrates no trace of Bradykinin ions (Fig. 8(b)).

Another example illustrating the softness of the AP-MALDI method is demonstrated by the data in Fig. 9 where the AP-MALDI spectrum of the PNN-82 molecules (the structure is shown on the inset in Fig. 9) is shown. It is interesting that we failed to get any molecular ions of these molecules using a conventional vacuum MALDI-TOF instrument since this molecule is very fragile for vacuum MALDI. In

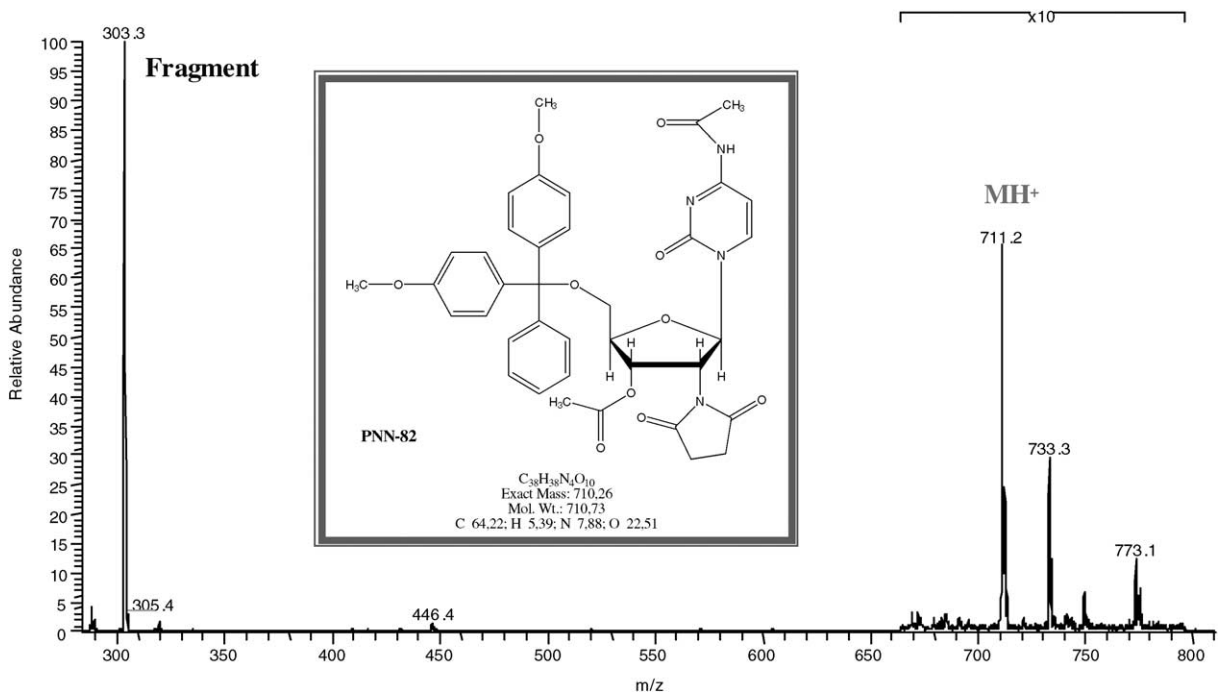

Fig. 9. AP-MALDI mass spectrum of PNN-82 molecules (1 pmol loaded) using DHB matrix. The structure of the molecules is shown on the inset.

contrast, AP-MALDI generates molecular ions although fragment ions are also present in abundant quantities. This result emphasizes the softness of the AP-MALDI method that was already reported in the very first publication on AP-MALDI.

3.4. Tryptic digest mixture analysis and MS/MS experiments

Proteome analysis is most commonly accomplished by the combination of 2D gel electrophoresis (or any other separation technique) and mass spectrometry. Proteins can be identified by analysis of peptide mixtures resulted from the digestion of individual gel spots. Adding tandem mass spectrometry (MS/MS) results in enormous additional information which is useful for protein identification. In addition, MS/MS itself is a powerful separation tool since a single peptide can be selected and fragmented in the presence of many other peptides.

In contrast to ESI, because of predominant use of TOF mass spectrometry with MALDI sources, it has not been easy to do tandem MS experiments on MALDI instruments. Only recently, true tandem MALDI instruments showed up on the market and AP-MALDI combined with an ion trap is the first candidate among them. In this work we demonstrate the usefulness of AP-MALDI for protein digest

Table 1
Fragments of protein digest mixtures observed in AP-MALDI mass spectra

Protein tryptic digest fragment	Peptide sequence	Measured mass (Da)	Calculated mass (Da)
Bovine serum albumin (cow)			
161–167	YLYEIAR	927.7	927.5
460–468	CCTKPESER	1052.7	1052.4
66–75	LVNELTEFAK	1163.9	1163.6
35–44	FKDLGEEHFK	1249.9	1249.6
402–412	HLVDEPQNLIK	1306.0	1305.7
106–117	ETYGDMADCCEK	1364.0	1364.4
298–309	LKECCDKPLLEK	1418.9	1418.7
360–371	RHPEYAVSVLLR	1440.2	1439.8
421–433	LGEYGFQNALIVR	1480.0	1479.8
437–451	KVPQVSTPTLVEVSR	1640.1	1639.9
242–256	LSQKFPKAEFVEVTK	1750.8	1750.9
281–297	ADLAKYICDNQDTISSK	1884.1	1884.9
Lysozyme (chicken)			
19–23	KVFGR	606.5	606.4
33–39	HGLDNYR	874.5	874.4
135–143	GTDVQAWIR	1045.6	1045.5
52–63	FESNFNTQATNR	1428.7	1428.7
64–79	NTDGSTDYGILQINSR	1753.8	1753.8
Myoglobin (horse)			
97–102	HKIPIK	735.5	735.4
134–139	ALELFR	748.5	748.4
146–153	YKELGFQG	941.4	941.5
32–42	LFTGHPETLEK	1271.7	1271.7
46–56	FKHLKTEAEMK	1361.7	1361.7
64–77	HGTVVLTALGGILK	1378.8	1378.8
119–133	HPGDFGADAQGAMTK	1502.7	1502.7
17–31	VAADIAGHGQEVLIR	1606.9	1606.9

The identification of peptides observed in AP-MALDI mass spectra was done using a SWISS-PROT database (http://ca.expasy.org/cgi-bin/peptide-mass.pl). Maximum number of missed cleavages was set to 2; all cysteins were in reduced form and monoisotopic masses were used to find the occurring amino acid residues giving peptide ion masses in the form of $[M + H]^+$.

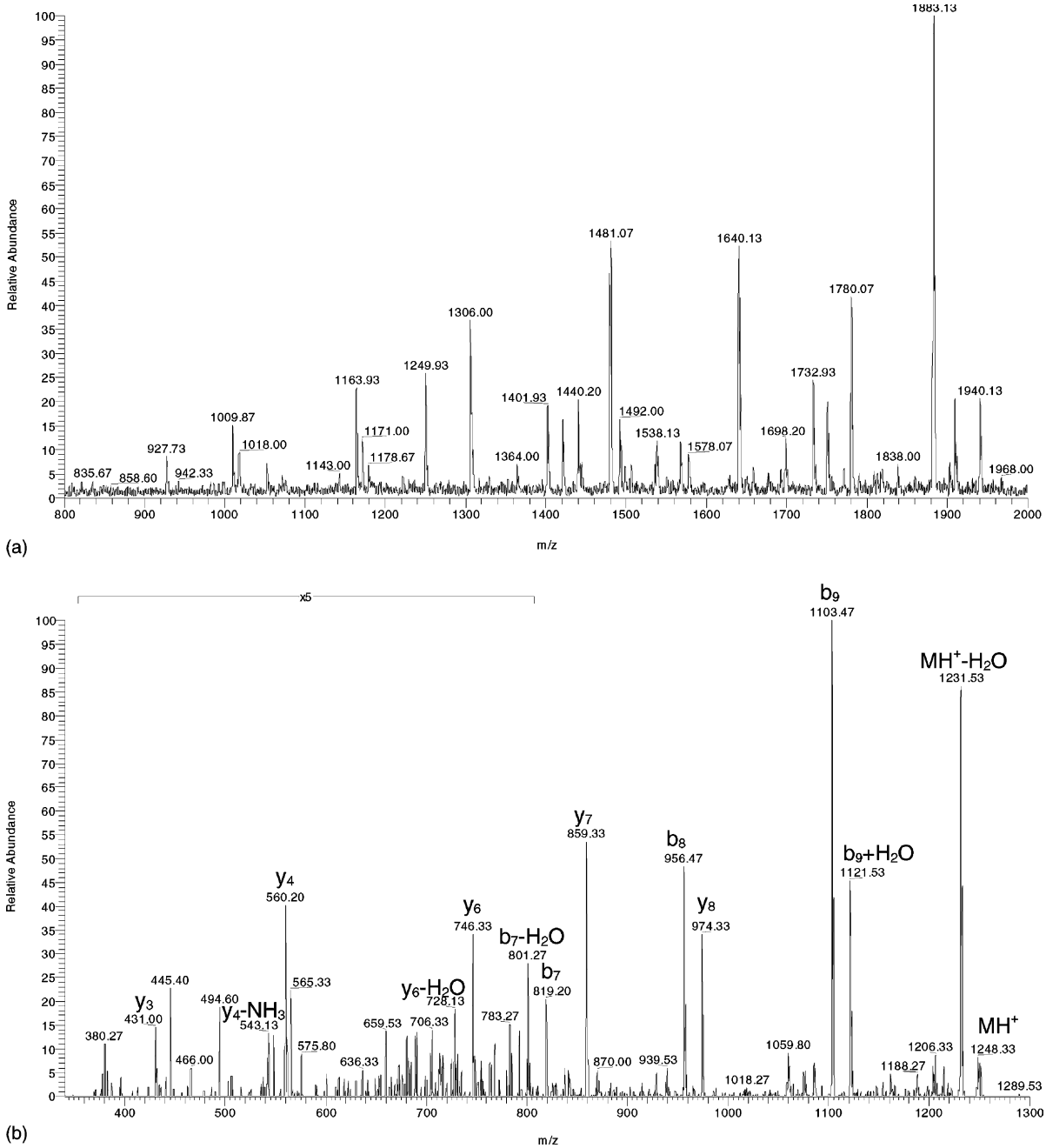

Fig. 10. The AP-MALDI mass spectrum from 250 fmol of bovine serum albumin tryptic digest (a) and MS/MS spectra of the fragment ion at *m*/*z* 1249 (b). CHCA was used as a matrix.

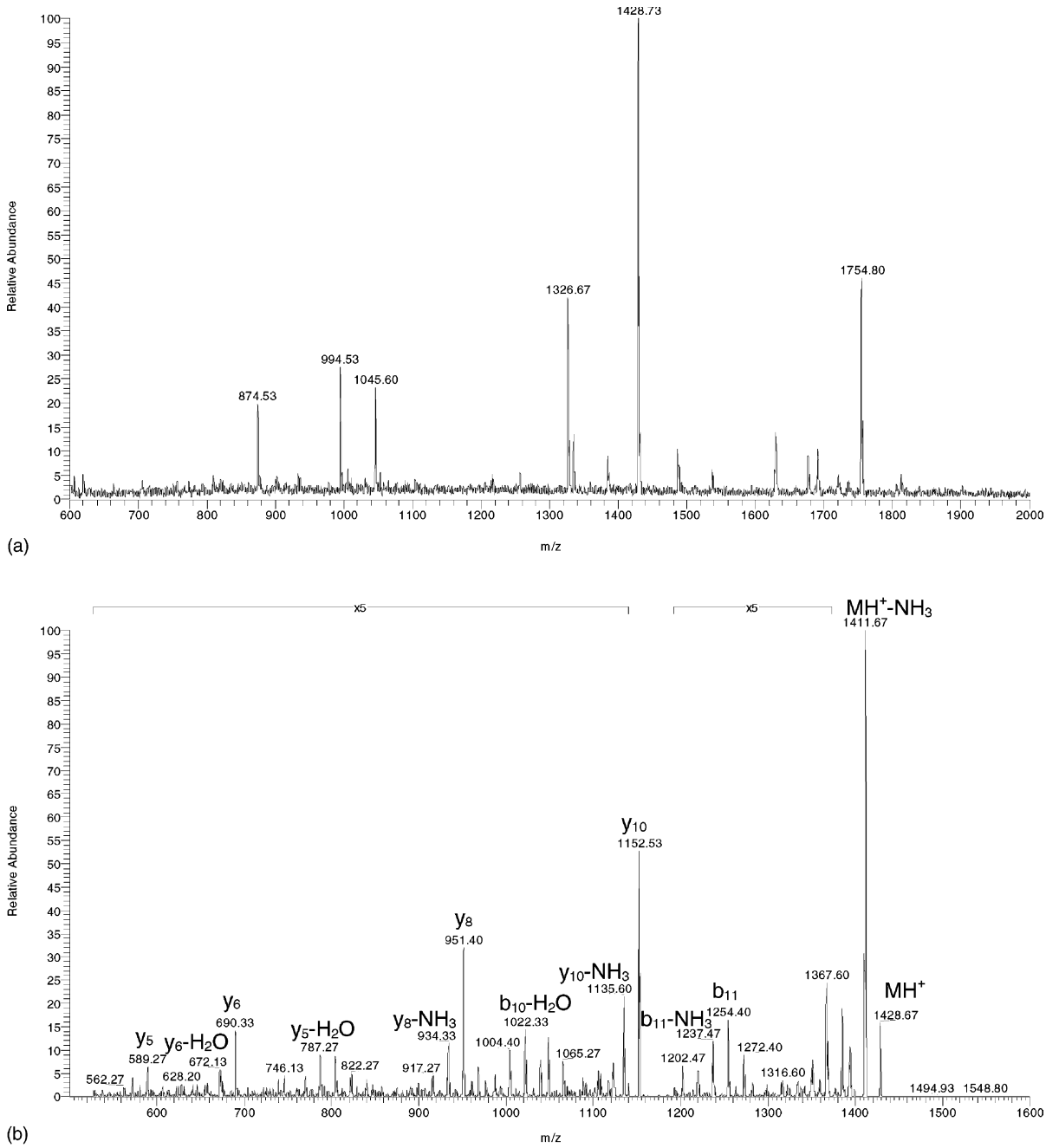

Fig. 11. The AP-MALDI mass spectrum from 250 fmol of lysozyme tryptic digest (a) and MS/MS spectra of the fragment ion at *m*/*z* 1428 (b). CHCA was used as a matrix.

analysis and the power of MS/MS for protein identification.

The AP-MALDI mass spectrum taken from 250 fmol of bovine serum albumin (BSA) tryptic digest is shown in Fig. 10(a). The results of the identification of peptides in the mixture using a SWISS-PROT database are presented in Table 1. The BSA fragments observed in the digest mixture and corresponding amino acid sequences are shown in the first and second columns, respectively. The greater specificity is provided by MS/MS experiments where additional fragments are generated in enormous quantities. As an example, the results of one such experiment are illustrated in Fig. 10(b) where the MS/MS spectrum for the 1249 Da peptide ion is shown. The peptide MS/MS fragment ions were identified using a PROSPECTOR

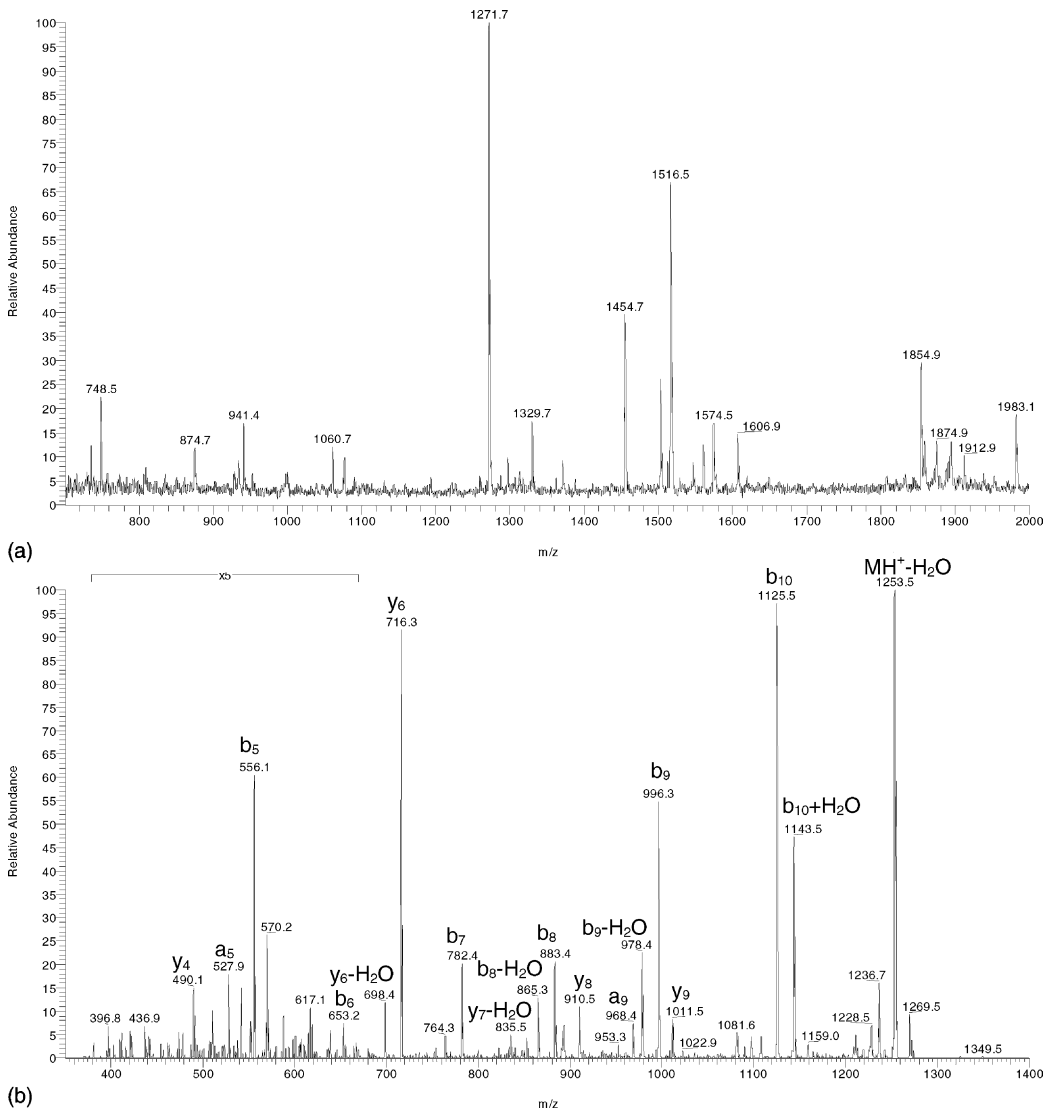

Fig. 12. The AP-MALDI mass spectrum from 250 fmol of myoglobin tryptic digest (a) and MS/MS spectra of the fragment ion at *m/z* 1271 (b). CHCA was used as a matrix.

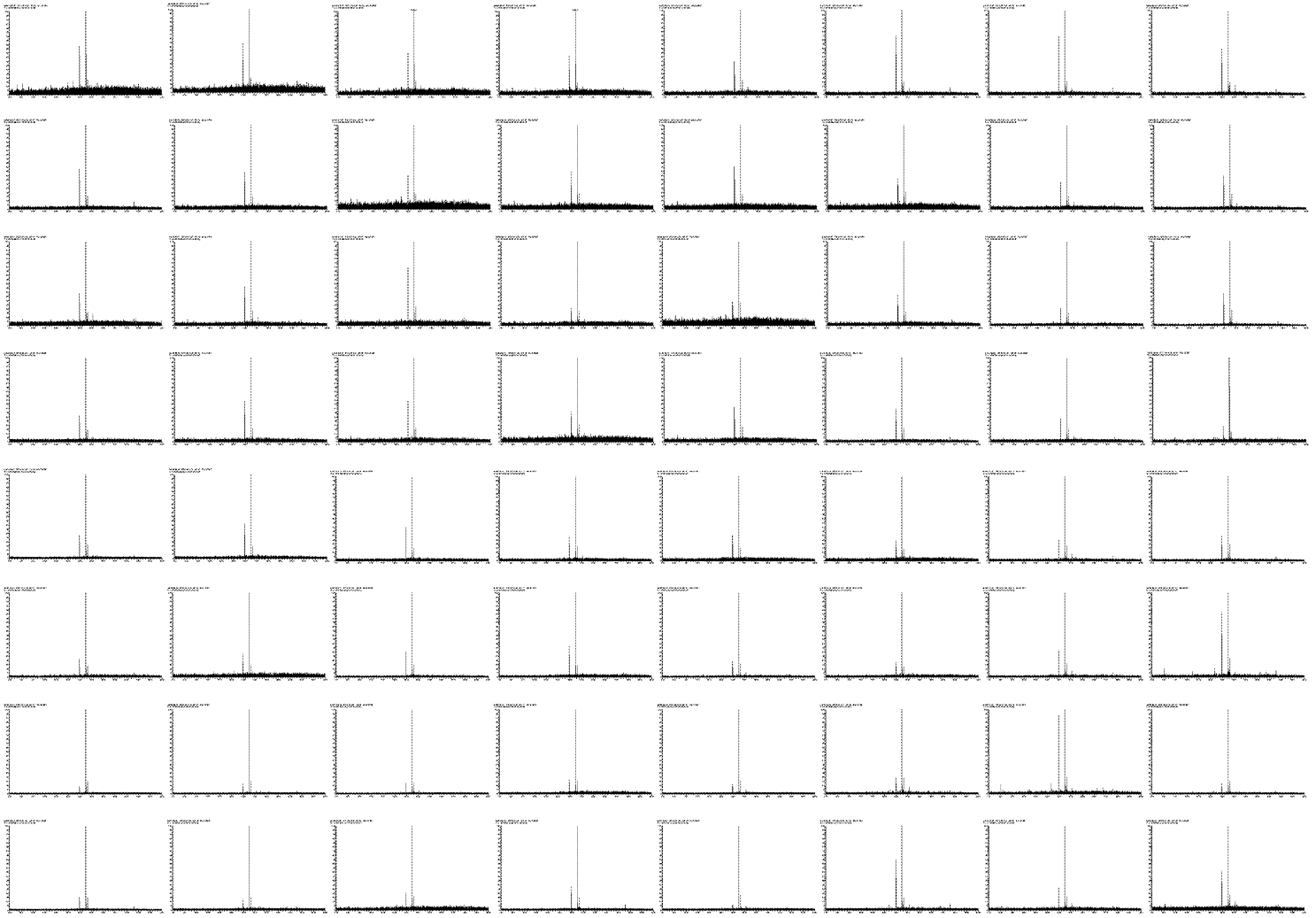

Fig. 13. The AP-MALDI mass spectra from 64 identical samples obtained in automated mode (100 femtomoles of Angiotensin I and Substance P in CHCA matrix were loaded in each sample).

software, developed by University of California at San Francisco (http://prospector.ucsf.edu) [35]. It is important to note that MS/MS experiments with singly-charged AP-MALDI ions produce a large number of meaningful fragment ions, in some cases leading to full peptide sequencing. (This was not apparent in advance since LCQ traps were originally designed to perform tandem MS experiments with ESI multiple-charged ions which are much easier to fragment.) One can see that the number of fragment ions generated in the MS/MS experiment of only one ion at *m*/*z* 1249 is comparable with that obtained in a normal digest mixture MS spectrum (Fig. 10(a)). This number can be increased significantly if all digest peptides undergo fragmentation in MS/MS experiments. These multiple MS/MS experiments can be done in automated mode (see below).

Another example of protein digest analysis is illustrated in Figs. 11(a) and 12(a) where respectively the AP-MALDI spectra of lysozyme and myoglobin tryptic digest mixtures are presented. The list of most intense protein digest ions identified from those spectra is shown in Table 1. The representative MS/MS spectra of 1428 and 1271 Da fragments from lysozyme and myoglobin digest mixtures are shown in Figs. 11(b) and 12(b), respectively.

3.5. High throughput analysis

The AP/MALDI source described here includes hardware and software required for high throughput analysis of sample arrays. Currently the target plate contains 64 (8 × 8) samples. Six such plates put in a special holder make a standard 384-sample microtiter plate that can be used for automated sample preparation using standard robotic techniques. In another version a 96 (12 × 8)-sample plate can be used for analysis and four of each can be combined to form a standard 384-sample microtiter plate. In this work, for demonstration purposes, 64 identical samples were loaded manually on a 64-sample plate. Every sample contained Angiotensin I and Substance P biomolecules (100 fmol each). Then, the LCQ's Xcalibur software was programmed to start every single spot MS analysis cycle from an external contact closure. In an automated sequence analysis mode, the AP/MALDI software provided a trigger signal for starting the Xcalibur analysis cycle at the beginning of the laser firing onto the sample. Then, the AP/MALDI software monitored the contact closure event provided by the Xcalibur software to stop firing the laser and move to the next sample. In this mode all 64 samples were analyzed without operator interference taking 30 s for data acquisition on each sample. The target plate moved along a spiral line during data acquisition to provide a fresh sample for every laser shot. The data from different samples were saved by the Xcalibur software in different files.

All 64 spectra obtained from every sample on the target plate are shown in Fig. 13. One can see that the peptide characteristic peaks are observed in all 64 spectra with high signal-to-noise ratio. Some variations in peptide peak intensities are typical for MALDI and in our AP-MALDI case are mostly due to the manual method of sample preparation used. The reproducibility of spectral data taken from the same sample is much higher than that obtained from different sample (data not shown). The use of robotic means for sample preparation can increase the sample position accuracy, its uniformity, and, thus, the data reproducibility. The intensity of all peaks in the spectra in Fig. 13 is quite enough for using those peaks as a precursor peak in effective MS/MS analysis. In the Xcalibur software, the MS/MS and $(MS)^n$ analysis can be done "on-the-fly" (the so-called data-dependent data acquisition) so that peaks for MS/MS experiments are chosen and MS/MS experiments are performed in real time without operator interference. The use of the AP/MALDI ion source for automated MS/MS analysis of real samples will be described in future works.

4. Conclusions

The atmospheric pressure MALDI is a new and extremely attractive alternative to known means for ionization of biological molecules such as ESI and conventional vacuum MALDI. The most important

features of AP-MALDI are its compatibility with ESI-MS instruments (the ESI and AP-MALDI sources can be replaced for a few minutes), its softness comparable to ESI, and its capability of tandem MS if it is interfaced with trap instruments. Integration of a sample target with *x–y* travel stages added high throughput capabilities to the AP-MALDI technique. The strength of this technique has been illustrated by numerous applications ranging from small molecule analysis to protein identification.

Future developments of the AP-MALDI technology may include increased sensitivity of the method, extending its mass range, and interfacing to a broader range of MS instruments including orthogonal TOF-MS.

Acknowledgements

This work was supported in part by a SBIR grant from the National Institutes of Health to Science and Engineering Services Inc., Burtonsville, MD, USA (1R43RR15331-01). The authors are also thankful to the reviewer for valuable comments.

References

[1] M. Yamashita, J.B. Fenn, J. Chem. Phys. 88 (1984) 4451.
[2] M. Karas, F. Hillenkamp, Anal. Chem. 60 (1988) 2299.
[3] K. Tanaka, Y. Ido, S. Akita, Y. Yoshida, T. Yoshida, Rapid Commun. Mass Spectrom. 2 (1988) 151.
[4] R.J. Cotter, Time-of-Flight Mass Spectrometry: Instrumentation and Applications in Biological Research, ACS Professional Reference Books, Washington, DC, 1997.
[5] W.C. Wiley, I.H. McLaren, Rev. Sci. Instrum. 26 (1955) 1150.
[6] S.M. Colby, T.B. King, J.P. Reilly, Rapid Commun. Mass Spectrom. 8 (1994) 865.
[7] R.M. Whittal, L. Li, Anal. Chem. 67 (1995) 1950.
[8] R.S. Brown, J.J. Lennon, Anal. Chem. 67 (1995) 1998.
[9] M.L. Vestal, P. Juhasz, S.A. Martin, Rapid Commun. Mass Spectrom. 9 (1995) 1044.
[10] B.A. Mamyrin, V.I. Karataev, D.V. Shmikk, V.A. Zagulin, Sov. Phys. JETP 37 (1973) 45.
[11] E. Nordhoff, A. Engendoh, R. Cramer, A. Overberg, B. Stahl, M. Karas, F. Hillenkamp, P.F. Crain, Rapid Commun. Mass Spectrom. 6 (1992) 771.
[12] U. Pieles, W. Zurcher, M. Schär, H.E. Moser, Nucl. Acids Res. 21 (1993) 3191.
[13] G.J. Currie, J.R. Yates, J. Am. Soc. Mass Spectrom. 4 (1993) 955.
[14] Y.-H. Lui, J. Bai, X. Liang, D.M. Lubman, Anal. Chem. 67 (1995) 3482.
[15] J. Bai, Y.-H. Lui, X. Liang, Y. Zhu, D.M. Lubman, Rapid Commun. Mass Spectrom. 9 (1995) 1172.
[16] A. Overberg, M. Karas, U. Bahr, R. Kaufmann, F. Hillenkamp, Rapid Commun. Mass Spectrom. 4 (1990) 293.
[17] S. Berkenkamp, C. Menzel, M. Karas, F. Hillenkamp, Rapid Commun. Mass Spectrom. 11 (1997) 1399.
[18] S. Niu, W. Zhang, B.T. Chait, J. Am. Soc. Mass Spectrom. 9 (1998) 1.
[19] S. Berkenkamp, F. Kirpekar, F. Hillenkamp, Science 281 (1998) 260.
[20] V.L. Talrose, M.D. Person, R.M. Whittal, F.C. Walls, A.L. Burlingame, M.A. Baldwin, Rapid Commun. Mass Spectrom. 13 (1999) 2191.
[21] V.V. Laiko, A.L. Burlingame, in: Proceedings of the Abstracts of the 4th International Symposium on Mass Spectrom, Health Life Sci., San Francisco, CA, 1998, p. 72.
[22] V.V. Laiko, M.A. Baldwin, A.L. Burlingame, Anal. Chem. 72 (2000) 652.
[23] V.V. Laiko, S.C. Moyer, R.J. Cotter, Anal. Chem. 72 (2000) 5239.
[24] J.H. Callahan, M. Galicia, A. Vertes, in: Proceedings of the 48th ASMS Conference on Mass Spectrom and Allied Topics, Long Beach, CA, 2000.
[25] R.M. Danell, G.L. Glish, in: Proceedings of the 48th ASMS Conference on Mass Spectrom and Allied Topics, Long Beach, CA, 2000.
[26] V.V. Laiko, N.I. Taranenko, V.D. Berkout, M.A. Yakshin, C.R. Prasad, H.S. Lee, V.M. Doroshenko, J. Am. Soc. Mass Spectrom. 13 (2002) 354.
[27] K. Hiraoka, S. Saito, J. Katsuragawa, I. Kudaka, Rapid Commun. Mass Spectrom. 12 (1998) 1170.
[28] I. Kudaka, T. Kojima, S. Saito, K. Hiraoka, Rapid Commun. Mass Spectrom. 14 (2000) 1558.
[29] A.N. Krutchinsky, A.V. Loboda, V.L. Spicer, R. Dworschak, W. Ens, K.G. Standing, Rapid Commun. Mass Spectrom. 12 (1998) 508.
[30] A. Loboda, A. Krutchinsky, V. Spicer, W. Ens, K. Standing, in: Proceedings of the 47th ASMS Conference on Mass Spectrom and Allied Topics, Dallas, TX, 1999.
[31] A. Verentchikov, I. Smirnov, M.L. Vestal, in: Proceedings of the 47th ASMS Conference on Mass Spectrom and Allied Topics, Dallas, TX, 1999.
[32] R.M. Danell, G.L. Glish, in: Proceedings of the 49th ASMS Conference on Mass Spectrom and Allied Topics, Chicago, IL, 2001.
[33] R.E. Kaiser, R.G. Cooks, G.C. Stafford, J.E.P. Syka, P.H. Hemberger, Int. J. Mass Spectrom. Ion Phys. 106 (1991) 79.
[34] B. Lin, J. Sunner, J. Am. Soc. Mass Spectrom. 5 (1994) 873.
[35] K.F. Clauser, P.R. Baker, A.L. Burlingame, Anal. Chem. 71 (1999) 2871.